
Filament Recycling and Sustained Contractile Flows in an Actomyosin Cortex

William McFadden¹, Jonathan Michaux², Patrick McCall³, Edwin Munro^{2,*}

1 Biophysical Sciences Program, University of Chicago, Chicago, IL, USA

2 Department of Molecular Genetics and Cell Biology, University of Chicago, Chicago, IL, USA

3 Department of Physics, University of Chicago, Chicago, IL, USA

* emunro@uchicago.edu

Abstract

Fill in abstract later.

Author Summary

In this paper, we develop and analyze a minimal model for 2D active networks based on the cortical cytoskeleton of eukaryotic embryos. Our model introduces a drag-like slip between cross-linked filaments as means to dissipate stored stress, generating a macroscopic effective viscosity. We further introduce an active friction to active stress from microscopic properties. We generate computational simulations based on the model, and demonstrate that active stress is sufficient to drive network contraction only temporarily. By introducing filament recycling, we are able to set up steady state flow profiles such those found in the cortex of developing embryos and migrating cells. The model is used to calculate phenomenological constants measured in prior experiments. Our analysis sheds insight on potential microscopic control parameters governing broad qualitative differences in 2D active networks.

Introduction

Active networks of cross-linked polymers are a class of materials with poorly understood but highly interesting properties. Cross-linked networks of cytoskeletal polymers have been a subject of great interest because of their importance as structural components of cells [2, 3].

The fluid-like deformability of actin networks is an important but often over-looked aspect of cell mechanics At long timescales, the purely elastic behavior of cross-linked networks gives way to fluid-like stress relaxation. Additionally, fluid-like flows have been observed in a number of cellular processes [27–32]. In *in vitro* studies, long timescale creep behaviors are thought to arise predominantly from the transient nature of filament binding for most biologically relevant cross-linkers [33–36]. While the importance of cross-link dynamics in determining the mechanical response of semi-flexible polymer networks has been known for at least 20 years [5], there is still a gap in our understanding of how microscopic cross-link unbinding relates to viscous flows.

Further introductory detail about the components of the actin cortex and how they turn over through actin recycling

Synopsis of mechanical picture and mentions of the theoretical and computational attempts to describe it The dependence of network rheology on cross-link unbinding is an active subject of theoretical research [21]. Several theoretical methods have addressed cross-link binding and unbinding directly [6, 21] in analytical approaches that allowed well-constrained fits for specific cross-linkers. These theories have therefore focused conceptually at the level of the cross-linked filament and were extended analytically to macroscopic networks. In another approach, modelers have taken cross-links as extended springlike structures [37] that are able to bind and unbind in simulated filament networks. Finally, other more ambitious simulations have even sought to interrogate the effects of cross-link unbinding in combination with the more complex mechanics of filament bundles [34, 38].

Ultimately, the complication of the many theoretical approaches that have been applied to this problem have made it difficult to distinguish what, if any, core physical mechanisms may be sufficient to explain the observed forms of stress relaxation. We believe that serious qualitative understanding can be generated by focusing on some of the common elements exhibited in the aforementioned literature.

Our model provides novel insight in to the importance of filament recycling in determining cortical flow rates Here, we introduce a coarse-grained representation of filament cross-linking in which cross-linked filaments which are able to slide past each other as molecular bonds form and rupture, akin to coarse-grained models of molecular friction [39–41]. This drag-like coupling has been shown to be an adequate approximation in the case of ionic cross-linking of actin [42, 43], and can be found in the theoretical basis of force-velocity curves for myosin bound filaments [44]. We propose that it will form a suitable bulk approximation in the presence of super molecular cross-links as well.

Importantly, this simplification allows us to extend our single polymer models to dynamical systems of larger network models for direct comparison between theory and modeling results. This level of coarse graining will therefore make it easier to understand classes of behavior for varying compositions of cross-linked filament networks. In addition, it allows us to compute a new class of numerical simulations efficiently, which gives us concrete predictions for behaviors in widely different networks with measurable dependencies on molecular details.

Finally, we also use this paper as a platform to present our modeling framework, which is publicly available at . We hope that making this model freely accessible and making our methodology transparent will enable other researchers to clearly understand our modeling framework and to build upon our findings.

Models

Asymmetric Filament Compliance

We consider individual filaments as chains of springs with relaxed length l_s . The orientations of neighboring springs are linearly coupled. Filaments can therefore be represented as a sequence of nodes with positions \mathbf{x}_i and nearest neighbor interactions of the form

$$|F_{i,i+1}|_e = -\mu_e \cdot \frac{|\mathbf{x}_{i+1} - \mathbf{x}_i| - l_s}{l_s} \quad (1)$$

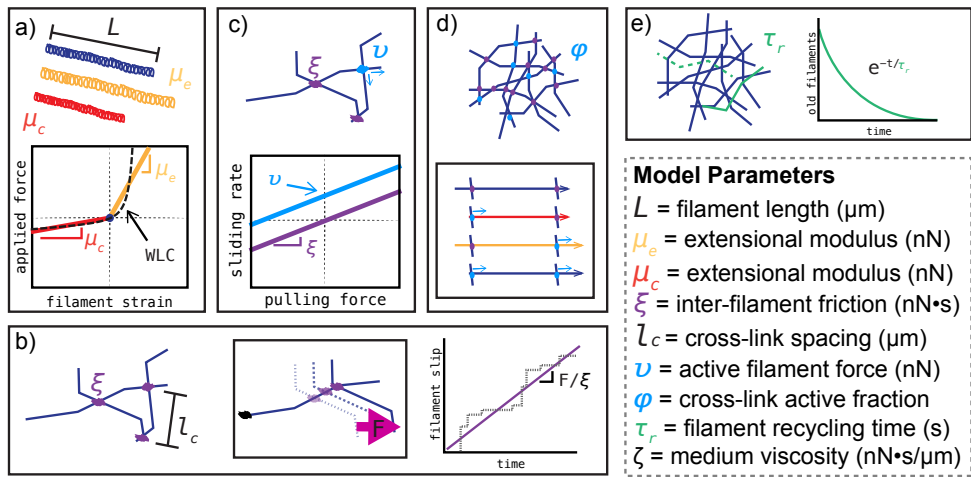


Figure 1. Schematic of modeling framework. a) Asymmetric filament compliance. Filaments have smaller spring constant for compression than for extension. b) Cross-link slip. Cross-links are coupled by an effective drag, such that their relative motion is proportional to any applied force. c) Motor activity. Filament activity manifests as a basal sliding rate even in the absence of an external force. d) Fractional activity. Only a subset of filament cross-links are active, resulting in differential force exertion along the filament. e) Filament recycling. Filaments are turned over at a constant rate, leading to a refreshing in the strain state of all filaments after a characteristic timescale.

$$|F_{i,i+1}|_c = -\mu_c \cdot \frac{|\mathbf{x}_{i+1} - \mathbf{x}_i| - l_s}{l_s} \quad (2)$$

where, μ represents an extensional modulus of a filament. Here, we take the extensional modulus as a composite quantities related to both filament and cross-linker compliance in a manner similar to a proposed effective medium theory [26]. In the limit of highly rigid cross-links and flexible filaments, our model reduces to the pure semi-flexible filament models of [12, 13]. In the opposite regime of nearly rigid filaments and highly flexible cross links, our method is still largely similar to the model of [26] in small strain regimes before any nonlinear cross link stiffening. However, in departure from those models, the magnitude of the force on interior cross-links in our model is still the same as those on the exterior. This is a simplification of the varying levels of strain that would actually be present in these cross-linkers as addressed in [26], but we choose to ignore the slight variation in favor of an approximated, global mean approach.

2D Network Formation

We choose to focus our attention on 2D networks both for their tractability as well as their relevance in the quasi-2D cytoskeletal cortex of many eukaryotic cells [27]. In addition, recent developments in 2D *in vitro* systems [45, 46], make 2D disordered models all the more interesting as a renewed focus of study.

We follow a mikado model approach by initializing a minimal network of connected unstressed linear filaments in a rectangular 2D domain. We generate 2D networks of these semi-flexible filaments by laying down straight lines of length, L , with random position and orientation. We then assume that some fixed fraction of overlapping filaments become cross-linked (defined in) at their point of overlap.

Although real cytoskeletal networks may form with non-negligible anisotropy, we focus on isotropically initialized networks for simplicity. We define the density using the average distance between cross-links along a filament, l_c . A simple geometrical argument can then be used to derive the number of filaments filling a domain as a function of L and l_c [12]. Here, we use the approximation that the number of filaments needed to tile a rectangular domain of size $W \times H$ is $2WH/Ll_c$, and that the length density is therefore $1/l_c$. In the absence of cross-link slip, we expect the network to form a connected solid with a well defined elastic modulus [12, 13].

Drag-like Coupling Between Overlapping Filaments

In contrast to previous models, we allow relaxation of the network's stored stress by letting the attachment points slip. We do this by replacing an elastic interaction between pairs of points along filaments with a drag-like coupling between filaments.

$$\mathbf{F}_{\text{drag}} = \xi \cdot \int ds (\mathbf{v}_i(\mathbf{s}) - \mathbf{v}_j(\mathbf{s})) p_{ij}(s) \quad (3)$$

Where $p_{ij}(s)$ represents the locational distribution of cross-link points (equal to 1 at locations of cross-links and 0 elsewhere) and $\mathbf{v}_i(\mathbf{s})$ and $\mathbf{v}_j(\mathbf{s})$ represent the velocities of the i th and j th filaments. This model assumes a linear relation between applied force and the velocity difference between attached filaments. Obviously, non-linearities can arise in the presence of force dependent detachment kinetics as well as non-linear force extension of cross-links. We address non-linear effects of stress induced unbinding in Appendix ???. Assuming inhomogeneities from non-linear effects are of second order, the motion for the entire network is governed by a dynamical equation of the form

$$\int ds (\zeta \mathbf{v}_i(\mathbf{s}) + \xi \sum_j (\mathbf{v}_i(\mathbf{s}) - \mathbf{v}_j(\mathbf{s})) p_{ij}(s)) = \mathbf{F}_i \quad (4)$$

Here, the first term in the integral is the filament's intrinsic drag through its embedding fluid, ζ , while the second comes from the drag-like coupling between filaments, ξ .

Active Coupling for Motor Driven Filament Interactions

To add motor activity we select a subset of cross-linked points and impart an additional force of magnitude v directed in the orientations of the individual filaments, \mathbf{u}_i . This leads to a modification of the equation of motion to

$$\int ds (\zeta \mathbf{v}_i(\mathbf{s}) + \xi \sum_j (\mathbf{v}_i(\mathbf{s}) - \mathbf{v}_j(\mathbf{s})) p_{ij}(s)) = \mathbf{F}_i + \mathbf{u}_i \cdot v \int ds \sum_j p_{ij}(s) q_{ij}(s) \quad (5)$$

In this formulation, only at the subset of points where $p_{ij}(s) = 1$ and $q_{ij}(s) = 1$ will there be a force imparted. In our simulations we let q_{ij} be selected randomly such that $\bar{q} = \phi$, where \bar{q} indicates the mean of q .

Filament Recycling as a model for rapid filament turnover

To simplify the complex biochemical changes that can give rise to actin filament polymerization and depolymerization, we chose to use simple filament appearance and disappearance as a lowest order model of filament recycling. In this sense the average lifetime of a filament between it's appearance and disappearance would be τ_r . In order

to do this without causing an unnecessary bias in the results, at a regularized interval $\tau_s < 0.01 \cdot \tau_r$, we selected τ_s/τ_r filaments, reset their extension or compression to 0, and relocated them to a random position and orientation. This has the effect of creating an approximately exponential decay in the number of old filaments over time.

System of Equations for Applied Stress

We model our full network as a coupled system of differential equations satisfying 5. Although the general mechanical response of this system may be very complex, we focus our attention on low frequency deformations and the steady-state creep response of the system to an applied stress. To do this we introduce a fixed stress, σ along the midline of our domain. This stress points in the direction, $\hat{\mathbf{x}}$, producing extensional stress.

Finally, we add a 0 velocity constraint at the far edges of our domain of interest. We assume that our network is in the "dry," low Reynold's number limit, where inertial effects are so small that we can equate our total force to 0. Therefore, we have a dynamical system of wormlike chain filaments satisfying

$$\int ds (\zeta \mathbf{v}_i(s) + \xi \sum_j (\mathbf{v}_i(s) - \mathbf{v}_j(s)) p_{ij}(s)) = \mathbf{F}_i + \mathbf{u}_i \cdot \mathbf{v} \int ds \sum_j p_{ij}(s) q_{ij}(s) + \sigma \hat{\mathbf{u}}(\mathbf{x}_i) \quad (6)$$

subject to constraints such that $\mathbf{v}_i(\mathbf{x})$ is 0 with $x = 0$. This results in an implicit differential equation for filament segments which can be discretized and integrated in time to produce a solution for the motion of the system.

Computational Simulation Method

We tested our analytical conclusions on a computational model. More technical details of the model can be found in the Appendix, but we summarize the main modeling points here.

We discretize the filaments such that the equations of motion becomes a coupled system of equations for the velocities of filament endpoints, \mathbf{x} . The drag-like force between overlapping filaments results in a coupling of the velocities of endpoints.

$$\mathbf{A} \cdot \dot{\mathbf{x}} = \mathbf{f}(\mathbf{x}) \quad (7)$$

where \mathbf{A} represents a coupling matrix between endpoints of filaments that overlap, and $\mathbf{f}(\mathbf{x})$ is the spring force between pairs of filament segment endpoints. We can then numerically integrate this system of equations to find the time evolution of the positions of all filament endpoints.

We generate a network by laying down filaments with random position and orientation within a domain of size D_x by D_y with periodic boundaries in the y-dimension. The external stress (shear or extensional/compressional) is applied to all filament endpoints falling within a fixed x-distance from the center of the domain. Finally, filament endpoints falling within a fixed x-distance from the edges of the domain are constrained to be nonmoving.

The nominal units for length, force, and time are μm , nN, and s, respectively. We explored parameter space around an estimate of biologically relevant parameter values, given in Table 1.

Table 1. Simulation Parameter Values

parameter	symbol	physiological estimate
extensional modulus	μ	$1nN$
bending modulus	κ	$10^{-3}nN \cdot \mu m$
cross-link drag coefficient	ξ	<i>unknown</i>
medium drag coefficient	ζ	$0.0005 \frac{nNs}{\mu m^2}$
filament length	L	$5\mu m$
cross-link spacing	l_c	$0.5\mu m$
domain size	D	$10 - 50\mu m$

Results and Discussion

Actin turnover and actomyosin contraction play crucial roles in preserving sustained cortical flows in C. elegans embryos

This will be a section where we introduce the problem with a bit of flow data as well as some data illustrating the disruption of flow in jasplakinolide treatment.

Near the end make a mention of the idealized model consisting of a contracting and an expanding domain. This will allow a segue to the next two sections.

Filament recycling prevents cortical tearing and modulates the viscous stress relaxation of filament networks under external stress

We first probed the effect of filament recycling on the network's passive response by imposing an external force on our simulated network. As shown in Figure 2 part a), by applying a force at the boundary of a patch of network, we induced a net strain. On short timescales the network responded mostly elastically by approaching a fixed strain γ_0 , similar to that predicted by [12]. However, on times longer than τ_c , we found that the network approached a steady linear strain rate, characterized by an effective viscosity, η . We were able to develop a simple theoretical description that captured the observed dependence.

$$\eta_c = \xi \left(\frac{L}{l_c} \right)^2 \quad (8)$$

It is interesting to note that as shown in Figure 2, the crossover time, τ_c is well described by the ratio of the effective viscosity, η_c , to the elastic modulus, $G_0 = \mu/l_c$.

Filament recycling allows persistent stress buildup in active networks

Next we tackled the case of a network with spatially isotropic motor activity. We found that our simulation axioms were able to produce transient contraction of a patch of free-floating network. As shown in Figure 3 a, the contraction extent was strongly dependent on the magnitudes of both the filament asymmetry and the motor activity scale. Additionally, contraction would only occur when there was fractional motor activity, $\phi < 1$, (see supplement). The contraction was able to take place over a time scale, τ_c , but on time scales much longer the contraction would stall and polarity sorting would begin to dominate.

Due to the long term polarity sorting and the fact that filament recycling would be difficult to incorporate into a moving material, we additionally analyzed the stress

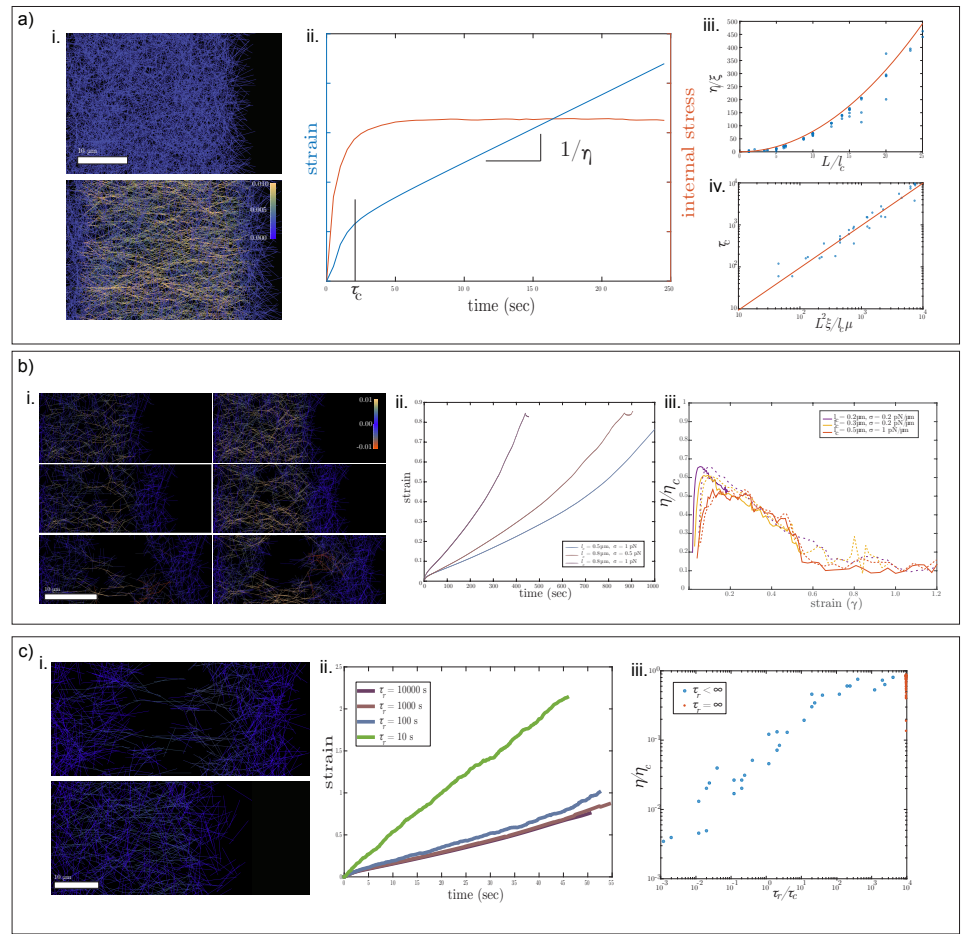


Figure 2. Filament recycling prevents cortical tearing and modulates the viscous stress relaxation of filament networks under external stress **a)** Network extension in the presence of cross-link slip alone. i. Example simulations of a network under and external applied extensional stress. ii. Example trace of the stress and strain buildup in an extending network. The network begins to behave purely viscously at τ_c , and the network deforms like a material with effective viscosity η_e . iii. The effective viscosity depends on the cross-link drag coefficient and the density of the network. iv. The timescale of the transition to viscous behavior has a characteristic dependence. **b)** Networks thin and tear at high strains. i. Example simulations of networks under extension at higher strains. ii. Example traces of networks in i. iii. Effective viscosity drops as networks are strained. **c)** Filament recycling rescues network tearing and modulates effective viscosity. i. Examples of same network under extension with and without recycling. ii. Illustration of the difference in strain for identical network setups in the presence of different filament recycling rates. iii. Master curve for the dependence of filament strain rate on the timescale of filament recycling relative to timescale of cross link slip.

buildup in a patch that was constrained to maintain its original area. As shown in Figure 3 b, the results showed a period of net stress due to an imbalance between larger stresses from extended filaments and smaller stresses from compressed filaments. After a characteristic timescale τ_a , the extensional stress peaks and begins to decrease while the

185
186
187
188

compressive stresses continue to build up resulting in the extensional and compressive stresses beginning to cancel each other. After another time period, τ_{eq} , the internal stresses become balanced and the net stress drops to approximately 0. The timescale and magnitude of the peak stresses agree with a qualitative expectation discussed later.

Upon the addition of filament recycling, we were able to find that the network maintained a nonzero net stress for times much longer than τ_{eq} . We refer to this as the steady state stress because based on our simulations it doesn't appear that this stress ever subsides, and duh. For similar network parameters as illustrated in Figure 3 c iii, we found that the steady state stress was well predicted by the comparison between the timescale of recycling, τ_r and that of peak activity, τ_a .

Filament recycling modulates the balance between active stress buildup and viscous stress relaxation to set the flow rate in polarized networks

Supporting Information

Acknowledgments

We would like to thank Shiladitya Banerjee and Patrick McCall for stimulating discussions.

References

1. Broedersz P C MacKintosh C F. Modeling semiflexible polymer networks. *Rev Mod Phys.* 2014 Jul;86:995–1036. Available from: <http://link.aps.org/doi/10.1103/RevModPhys.86.995>.
2. Fletcher DA, Mullins RD. Cell mechanics and the cytoskeleton. *Nature.* 2010 01;463(7280):485–492. Available from: <http://dx.doi.org/10.1038/nature08908>.
3. Salbreux G, Charras G, Paluch E. Actin cortex mechanics and cellular morphogenesis. *Trends in Cell Biology.* 2012;22(10):536 – 545. Available from: <http://www.sciencedirect.com/science/article/pii/S0962892412001110>.
4. Stamenovic D. Cell Mechanics: Two regimes, maybe three? *Nat Mater.* 2006 08;5(8):597–598. Available from: <http://dx.doi.org/10.1038/nmat1700>.
5. Wachsstock DH, Schwarz WH, Pollard TD. Cross-linker dynamics determine the mechanical properties of actin gels. *Biophysical Journal.* 1994;66(3, Part 1):801 – 809. Available from: <http://www.sciencedirect.com/science/article/pii/S0006349594808562>.
6. Broedersz CP, Depken M, Yao NY, Pollak MR, Weitz DA, MacKintosh FC. Cross-Link-Governed Dynamics of Biopolymer Networks. *Phys Rev Lett.* 2010 Nov;105:238101. Available from: <http://link.aps.org/doi/10.1103/PhysRevLett.105.238101>.
7. Tharmann R, Claessens MMAE, Bausch AR. Viscoelasticity of Isotropically Cross-Linked Actin Networks. *Phys Rev Lett.* 2007 Feb;98:088103. Available from: <http://link.aps.org/doi/10.1103/PhysRevLett.98.088103>.

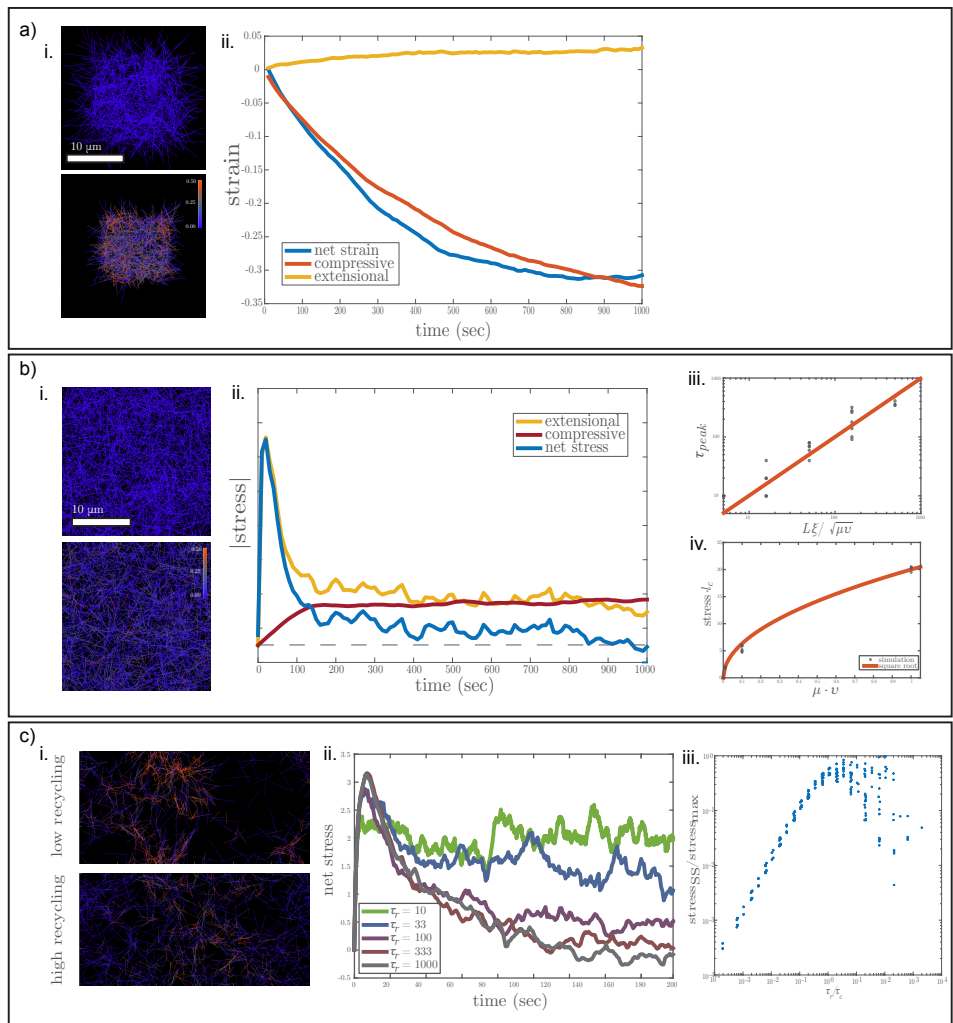


Figure 3. Filament recycling allows persistent active stress buildup in active networks. **a)** Network contraction. i. Example of an active network contracting. ii. Traces of total network strain and internal strain of filaments. **b)** Internal stress buildup is only transient. i. Example simulation of an active network building up internal stress while maintaining a constant area. ii. Traces of stress buildup. iii. Timescale of stress buildup. iv. Peak stress depends on myosin activity and filament stiffness. **c)** Filament recycling allows for steady state stress buildup. i. Example simulations of networks with fast and slow rates of recycling. ii. Traces of net stress for with different recycling timescales; faster recycling prevents the stress from relaxing entirely. iii. Steady state stress depends on the recycling time relative to the crossly relaxation time.

8. Gardel ML, Shin JH, MacKintosh FC, Mahadevan L, Matsudaira P, Weitz DA. Elastic Behavior of Cross-Linked and Bundled Actin Networks. *Science*. 2004;304(5675):1301–1305. Available from: <http://www.sciencemag.org/content/304/5675/1301.abstract>.
9. Marko JF, Siggia ED. Stretching DNA. *Macromolecules*. 1995;28(26):8759–8770. Available from: <http://dx.doi.org/10.1021/ma00130a008>.

-
10. Doi M, Edwards SF. *The Theory of Polymer Dynamics*. Oxford University Press, USA; 1986. Available from: <http://www.amazon.com/exec/obidos/redirect?tag=citeulike07-20&path=ASIN/0198520336>.
 11. Morse DC. Viscoelasticity of Concentrated Isotropic Solutions of Semiflexible Polymers. 2. Linear Response. *Macromolecules*. 1998;31(20):7044–7067. Available from: <http://dx.doi.org/10.1021/ma980304u>.
 12. Head DA, Levine AJ, MacKintosh FC. Deformation of Cross-Linked Semiflexible Polymer Networks. *Phys Rev Lett*. 2003 Sep;91:108102. Available from: <http://link.aps.org/doi/10.1103/PhysRevLett.91.108102>.
 13. Wilhelm J, Frey E. Elasticity of Stiff Polymer Networks. *Phys Rev Lett*. 2003 Sep;91:108103. Available from: <http://link.aps.org/doi/10.1103/PhysRevLett.91.108103>.
 14. Storm C, Pastore JJ, MacKintosh FC, Lubensky TC, Janmey PA. Nonlinear elasticity in biological gels. *Nature*. 2005 May;435(7039):191–194. Available from: <http://dx.doi.org/10.1038/nature03521>.
 15. Ward SMV, Weins A, Pollak MR, Weitz DA. Dynamic Viscoelasticity of Actin Cross-Linked with Wild-Type and Disease-Causing Mutant alpha-Actinin-4. *Biophysical Journal*. 2008;95(10):4915 – 4923. Available from: <http://www.sciencedirect.com/science/article/pii/S0006349508786302>.
 16. Lieleg O, Claessens MMAE, Bausch AR. Structure and dynamics of cross-linked actin networks. *Soft Matter*. 2010;6:218–225. Available from: <http://dx.doi.org/10.1039/B912163N>.
 17. Gardel ML, Nakamura F, Hartwig J, Crocker JC, Stossel TP, Weitz DA. Stress-Dependent Elasticity of Composite Actin Networks as a Model for Cell Behavior. *Phys Rev Lett*. 2006 Mar;96:088102. Available from: <http://link.aps.org/doi/10.1103/PhysRevLett.96.088102>.
 18. Gardel ML, Nakamura F, Hartwig JH, Crocker JC, Stossel TP, Weitz DA. Prestressed F-actin networks cross-linked by hinged filamins replicate mechanical properties of cells. *Proceedings of the National Academy of Sciences of the United States of America*. 2006;103(6):1762–1767. Available from: <http://www.pnas.org/content/103/6/1762.abstract>.
 19. Kasza KE, Broedersz CP, Koenderink GH, Lin YC, Messner W, Millman EA, et al. Actin Filament Length Tunes Elasticity of Flexibly Cross-Linked Actin Networks. *Biophysical Journal*. 2015/03/12;99(4):1091–1100. Available from: [http://www.cell.com/biophysj/abstract/S0006-3495\(10\)00737-X](http://www.cell.com/biophysj/abstract/S0006-3495(10)00737-X).
 20. Lin YC, Broedersz CP, Rowat AC, Wedig T, Herrmann H, MacKintosh FC, et al. Divalent Cations Crosslink Vimentin Intermediate Filament Tail Domains to Regulate Network Mechanics. *Journal of Molecular Biology*. 2010;399(4):637 – 644. Available from: <http://www.sciencedirect.com/science/article/pii/S0022283610004420>.
 21. Müller KW, Bruinsma RF, Lieleg O, Bausch AR, Wall WA, Levine AJ. Rheology of Semiflexible Bundle Networks with Transient Linkers. *Phys Rev Lett*. 2014 Jun;112:238102. Available from: <http://link.aps.org/doi/10.1103/PhysRevLett.112.238102>.

22. Cyron CJ, Müller KW, Bausch AR, Wall WA. Micromechanical simulations of biopolymer networks with finite elements. *Journal of Computational Physics*. 2013;244(0):236 – 251. Multi-scale Modeling and Simulation of Biological Systems. Available from: <http://www.sciencedirect.com/science/article/pii/S0021999112006262>.
23. Koenderink GH, Dogic Z, Nakamura F, Bendix PM, MacKintosh FC, Hartwig JH, et al. An active biopolymer network controlled by molecular motors. *Proceedings of the National Academy of Sciences of the United States of America*. 2009 09;106(36):15192–15197. Available from: <http://www.ncbi.nlm.nih.gov/pmc/articles/PMC2741227/>.
24. Heussinger C, Schaefer B, Frey E. Nonaffine rubber elasticity for stiff polymer networks. *Phys Rev E*. 2007 Sep;76:031906. Available from: <http://link.aps.org/doi/10.1103/PhysRevE.76.031906>.
25. Wyart M, Liang H, Kabla A, Mahadevan L. Elasticity of Floppy and Stiff Random Networks. *Phys Rev Lett*. 2008 Nov;101:215501. Available from: <http://link.aps.org/doi/10.1103/PhysRevLett.101.215501>.
26. Broedersz CP, Storm C, MacKintosh FC. Effective-medium approach for stiff polymer networks with flexible cross-links. *Phys Rev E*. 2009 Jun;79:061914. Available from: <http://link.aps.org/doi/10.1103/PhysRevE.79.061914>.
27. Mayer M, Depken M, Bois JS, Julicher F, Grill SW. Anisotropies in cortical tension reveal the physical basis of polarizing cortical flows. *Nature*. 2010 09;467(7315):617–621. Available from: <http://dx.doi.org/10.1038/nature09376>.
28. Hird SN, White JG. Cortical and cytoplasmic flow polarity in early embryonic cells of *Caenorhabditis elegans*. *The Journal of Cell Biology*. 1993;121(6):1343–1355. Available from: <http://jcb.rupress.org/content/121/6/1343.abstract>.
29. Bray D, White J. Cortical flow in animal cells. *Science*. 1988;239(4842):883–888. Available from: <http://www.sciencemag.org/content/239/4842/883.abstract>.
30. Hochmuth RM. Micropipette aspiration of living cells. *Journal of Biomechanics*. 2000;33(1):15 – 22. Available from: <http://www.sciencedirect.com/science/article/pii/S002192909900175X>.
31. Evans E, Yeung A. Apparent viscosity and cortical tension of blood granulocytes determined by micropipet aspiration. *Biophysical Journal*. 1989 07;56(1):151–160. Available from: <http://www.ncbi.nlm.nih.gov/pmc/articles/PMC1280460/>.
32. Bausch AR, Zieman F, Boulbitch AA, Jacobson K, Sackmann E. Local Measurements of Viscoelastic Parameters of Adherent Cell Surfaces by Magnetic Bead Microrheometry. *Biophysical Journal*. 1998;75(4):2038 – 2049. Available from: <http://www.sciencedirect.com/science/article/pii/S0006349598776465>.
33. Lieleg O, Claessens MMAE, Luan Y, Bausch AR. Transient Binding and Dissipation in Cross-Linked Actin Networks. *Phys Rev Lett*. 2008 Sep;101:108101. Available from: <http://link.aps.org/doi/10.1103/PhysRevLett.101.108101>.

-
34. Lieleg O, Schmoller KM, Claessens MMAE, Bausch AR. Cytoskeletal Polymer Networks: Viscoelastic Properties are Determined by the Microscopic Interaction Potential of Cross-links. *Biophysical Journal*. 2009;6;96(11):4725–4732. Available from: <http://www.sciencedirect.com/science/article/pii/S0006349509007589>.
35. Yao NY, Becker DJ, Broedersz CP, Depken M, MacKintosh FC, Pollak MR, et al. Nonlinear Viscoelasticity of Actin Transiently Cross-linked with Mutant alpha-Actinin-4. *Journal of Molecular Biology*. 2011;411(5):1062 – 1071. Available from: <http://www.sciencedirect.com/science/article/pii/S0022283611007376>.
36. Liu J, Koenderink GH, Kasza KE, MacKintosh FC, Weitz DA. Visualizing the Strain Field in Semiflexible Polymer Networks: Strain Fluctuations and Nonlinear Rheology of F-Actin Gels. *Phys Rev Lett*. 2007 May;98:198304. Available from: <http://link.aps.org/doi/10.1103/PhysRevLett.98.198304>.
37. Kim T, Hwang W, Kamm RD. Dynamic Role of Cross-Linking Proteins in Actin Rheology. *Biophysical Journal*. 2011;101(7):1597–1603. Available from: <http://www.ncbi.nlm.nih.gov/pmc/articles/PMC3183755/>.
38. Lieleg O, Bausch AR. Cross-Linker Unbinding and Self-Similarity in Bundled Cytoskeletal Networks. *Phys Rev Lett*. 2007 Oct;99:158105. Available from: <http://link.aps.org/doi/10.1103/PhysRevLett.99.158105>.
39. Vanossi A, Manini N, Urbakh M, Zapperi S, Tosatti E. *Colloquium : Modeling friction: From nanoscale to mesoscale*. *Rev Mod Phys*. 2013 Apr;85:529–552. Available from: <http://link.aps.org/doi/10.1103/RevModPhys.85.529>.
40. Spruijt E, Sprakel J, Lemmers M, Stuart MAC, van der Gucht J. Relaxation Dynamics at Different Time Scales in Electrostatic Complexes: Time-Salt Superposition. *Phys Rev Lett*. 2010 Nov;105:208301. Available from: <http://link.aps.org/doi/10.1103/PhysRevLett.105.208301>.
41. Filippov AE, Klafter J, Urbakh M. Friction through Dynamical Formation and Rupture of Molecular Bonds. *Phys Rev Lett*. 2004 Mar;92:135503. Available from: <http://link.aps.org/doi/10.1103/PhysRevLett.92.135503>.
42. Ward A, Hilitski F, Schwenger W, Welch D, Lau AWC, Vitelli V, et al. Solid friction between soft filaments. *Nat Mater*. 2015 03;advance online publication:–. Available from: <http://dx.doi.org/10.1038/nmat4222>.
43. Chandran PL, Mofrad MRK. Averaged implicit hydrodynamic model of semiflexible filaments. *Phys Rev E*. 2010 Mar;81:031920. Available from: <http://link.aps.org/doi/10.1103/PhysRevE.81.031920>.
44. Banerjee S, Marchetti MC, Müller-Nedebock K. Motor-driven dynamics of cytoskeletal filaments in motility assays. *Phys Rev E*. 2011 Jul;84:011914. Available from: <http://link.aps.org/doi/10.1103/PhysRevE.84.011914>.
45. Murrell MP, Gardel ML. F-actin buckling coordinates contractility and severing in a biomimetic actomyosin cortex. *Proceedings of the National Academy of Sciences*. 2012;109(51):20820–20825. Available from: <http://www.pnas.org/content/109/51/20820.abstract>.
46. Sanchez T, Chen DTN, DeCamp SJ, Heymann M, Dogic Z. Spontaneous motion in hierarchically assembled active matter. *Nature*. 2012 11;491(7424):431–434. Available from: <http://dx.doi.org/10.1038/nature11591>.